Investigation of surface plasmon biosensing using gold nanoparticles enhanced ellipsometry

Rakesh Singh Moirangthem,[1,2,3] Yia-Chung Chang,[1,*] and Pei-Kuen Wei[1,4]

[1]*Research Centre for Applied Sciences, Academia Sinica, Taipei 115, Taiwan*

[2]*Nano Science and Technology Program, TIGP, Academia Sinica, Taipei 115, Taiwan*

[3]*Department of Engineering and System Science, National Tsing Hua University, Hsinchu 300, Taiwan*

[4]*e-mail: pkwei@gate.sinica.edu.tw*

**Corresponding author: yiachang@gate.sinica.edu.tw*

Received October 26, 2010; revised January 19, 2011; accepted February 2, 2011;
posted February 3, 2011 (Doc. ID 137163); published March 1, 2011

We present a label-free, nondestructive and high sensitivity biosensor by using the phase information of a gold nanoparticles enhanced ellipsometry signal. The refractive index (RI) resolution from ellipsometric phase information is of the order of 1.6×10^{-6} RI units. Furthermore, spectroscopic and dynamic measurements show substantial change in the phase signal when biomolecules are coated on gold nanoparticles. The detection limit of our proposed technique is up to ~18 pM concentration of the target biomolecules.

OCIS codes: 250.5403, 260.2130, 280.1415, 280.4788.

Colloidal gold nanoparticles are becoming very popular in the areas of biological sensing and diagnostic applications due to their ease of preparation, ready bioconjugation, and ability to help achieve subwavelength resolution in label-free optical detection [1–3]. When light interacts with metallic nanoparticles much smaller than the incident wavelength, the incident electric field causes electron clouds to oscillate coherently relative to the nuclear framework of the nanoparticle. The frequency at which the maximal response due to the charge oscillation in the metallic nanoparticle occurs is defined as the localized surface plasmon resonance (LSPR) frequency. The resonance frequency is highly sensitive to the nanoparticle size and shape and to the interparticle distance and refractive indices of the surrounding materials [4,5]. The chip-based LSPR sensing scheme has been demonstrated by many groups by immobilizing gold nanoparticles (AuNPs) on a functionalized glass substrate and monitoring the change in height and wavelength of the LSPR peak due to solvents or polymers of different refractive indices in the surrounding environment of the AuNPs [4,6]. In this optical detection scheme, AuNPs are acting as transducers that convert small changes in the local refractive index (RI) into change in absorption amplitude and shift in resonance wavelength. The phase detection of the reflected light from metal thin film under the SPR condition for improving the sensitivity has been discussed [7]. However, the phase associated with the reflected light from the random distribution of metallic nanoparticles, which could carry useful information about the biomolecules adsorbed on the surface has not been analyzed so far to our knowledge. Recently, an optical phase detection scheme based on the grating coupled SPR sensor and gold nanoresonators has been reported. However, neither investigation extended its work to studies of biomolecular interactions [8,9]. Also, the fabrication of these metallic nanostructures using electron beam lithography is very expensive, time-consuming, and difficult to implement for commercialization. In this Letter, we present a phase detection scheme to study biomolecular interaction based on ellipsometry by using self-synthesized AuNPs immobilized on a functionalized glass substrate integrated with a custom-made flow cell. The simultaneous measurements of the ellipsometric parameters Ψ and Δ (which are the magnitude and phase of the ratio of the complex reflectivities for the *p*- and *s*-polarized waves) provide not only the relative magnitude but also the phase over the full spectral range, which leads to extra information about the optical properties of the sample under investigation. The details about ellipsometry can be found elsewhere [10]. Such an LSPR enhanced ellipsometry signal can be used for label-free biodetection with very high sensitivity. The ellipsometry setup used in our experiment is based on the commercially available variable angle spectroscopic ellipsometry (VASE, J.A. Woollam Company, USA) equipped with a BK7 dove prism and a custom-built microfluidic flow cell as shown in Fig. 1(a).

Measurements were performed at a fixed angle of incidence, i.e., at the total internal reflection angle for light

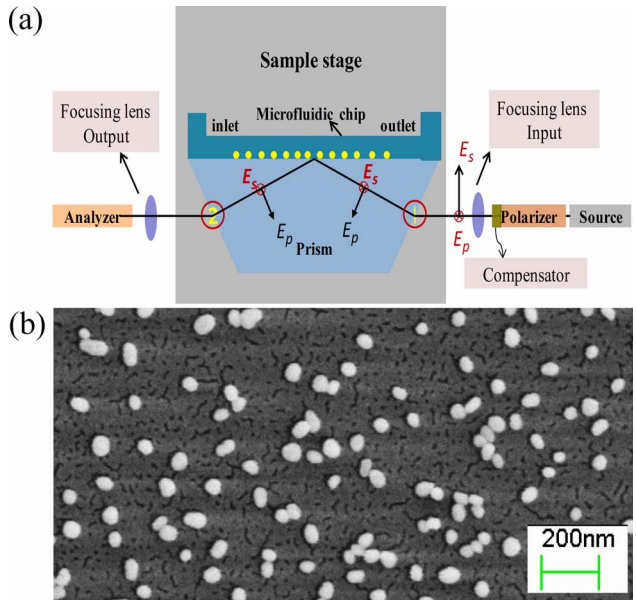

Fig. 1. (Color online) (a) Schematic diagram of our experimental setup and (b) SEM image of AuNPs on glass substrate.

propagation in a dove prism, ~72.8° (with a weak wavelength dependence) over the full spectral range from 400 nm to 1000 nm. Furthermore, a single axis alignment of optical components simplifies the complicated and high precision optical alignment procedure, and the focusing lens module helps to check the sample uniformity over different regions on the sample surface. Though the present experimental setup is done with a commercial instrument, the idea can be used when developing a standalone optical instrument for sensing applications. To carry out the experiment in an aqueous medium, a microfluidic flow cell is prepared with a central chamber by sandwiching acrylic plastic between two microscopic glass slides with inlet and outlet valves. The bottom glass slide attached to the microfluidic flow cell is replaced by a AuNPs immobilized glass substrate in optical contact with the prism where the light is internally reflected. An index matching liquid was used to remove the air gap at the prism–slide interference. AuNPs were prepared by sodium citrate (Sigma Aldrich, USA) reduction of chloroauric acid ($H[AuCl_4]$) solution (Sigma Aldrich) as reported earlier [11]. For the sample preparation, the glass substrates (Gold Seal, USA) were cleaned by piranha solution (70% H_2SO_4:30%H_2O_2), followed by rinsing with ultrapure water, and further cleaned in an ultrasound bath with acetone and isopropyl solution for 20 min each. The cleaned glass substrates were rinsed with water and dried in an oven prior to salinization. Surface modification of the glass substrate was done by immersing it in a 10% (volume in volume) solution of (3-aminopropyl) triethoxysaline (APTES, Sigma Aldrich) in anhydrous ethanol for 20 min, rinsed five times in ethanol with sonication and dried at 120 °C for 2 h. The AuNPs were poured on the silanized glass surface for 24 h in a humid environment to avoid the evaporation of the colloidal AuNPs solution from the surface and to ensure complete coverage to minimize variations in the sensitivity between different batches of the nanoparticles immobilized on the substrate. AuNPs with a mean diameter of 45 nm were chosen for our study because sizes ranging from 35–45 nm in diameter exhibit maximum sensitivity to the change of the bulk RI as reported earlier [4]. The scanning electron microscope (SEM) image of the AuNPs immobilized on the glass substrate is shown in Fig. 1(b). The reflection magnitude and phase response of AuNPs to changes in a surrounding medium with different refractive indices are shown in Fig. 2. The dip appearing at 540 nm for the Ψ spectra corresponds to the LSPR peak of the AuNPs where the reflection of the *p*-polarized light shows a minimum, and, at this particular wavelength, the phase signal (as it appears in the Δ spectra) has the steepest slope. Also, a typical LSPR response to the changes in the local surrounding medium can be seen in the Ψ spectra. Compared with the reflectance spectra (not shown), we found that the dip appearing in the Δ spectra in Fig. 2(b) occurs at the wavelength where the reflectance for the *s*-polarized light is a minimum, which shows the highest sensitivity to the changes in local surrounding media. Theoretical analysis will further help to gain more understanding about the interaction between the nanoparticles and the media, which is beyond the scope of the present investigation, and detailed theory can be found elsewhere [12].

As can be seen from Figs. 2(a) and 2(b), the phase response of the ellipsometric signal, Δ, is more pronounced than Ψ in the spectroscopic measurements. The bulk sensitivity of the AuNPs' base biosensor can be determined by measuring the phase signal change at the spectral position (575 nm) where it gives maximum response to changes in the surrounding medium. The RI values for different glycerol–water mixtures shown in Fig. 2 were measured using a refractometer (Misco, USA). The calculated sensitivity obtained from the slope over three different samples is shown in Fig. 2(c). The absolute value of the highest sensitivity obtained from our measurement is $612 \pm 22°$/RIU, assuming the phase measurement accuracy in a scheme with a fixed angle of incidence at a level of about 0.001° as adopted in the literature [9,13]. The obtained RI resolution for the present sensor based on phase signal is 1.63×10^{-6} RIU, which is comparable to a commercial SPR machine with high precision angular resolution [for example, SPR-Navi (BioNavis Ltd., Finland)] or a complicated interferometric SPR sensor [14,15]. In Fig. 2(c), the sensitivity variation among three different samples prepared under similar conditions may arise from the different aggregations or concentrations of the AuNPs in these samples. Therefore, it is necessary to calibrate every batch of samples by measuring the bulk sensitivity. The obtained bulk sensitivity can be used as a calibration to determine the detection limit and concentration of biomolecules in the subsequent biological experiments. The high sensitivity of the AuNPs' enhanced ellipsometry signal can be used for label-free biodetection of protein–protein interaction. In this demonstration, we measured the interaction between bovine serum albumin (BSA) and anti-BSA. BSA and anti-BSA (Sigma Aldrich, USA) were diluted in a 1× phosphate buffer saline (PBS, pH 7.4) buffer (UniRegion Bio-Tech, Taiwan) with concentrations of 50 μM

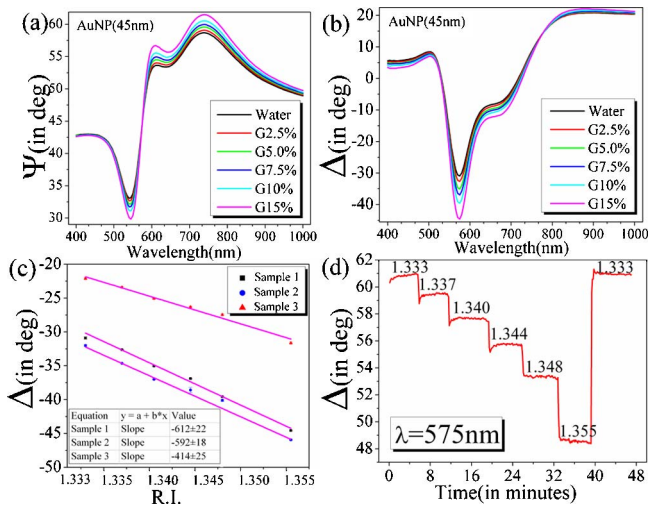

Fig. 2. (Color online) Spectral response of the ellipsometric parameters for (a) Ψ and (b) Δ for glycerol–water mixtures with various RIs; (c) changes of phase signal, Δ, and (d) dynamic response measured at fixed wavelength (575 nm) with varying RIs (δn) of glycerol–water mixtures. Error bars in Fig. 2(c) were determined from five independent measurements at the same spot for a given sample, and slopes with the standard deviation obtained from linear fitting of the data points are also given.

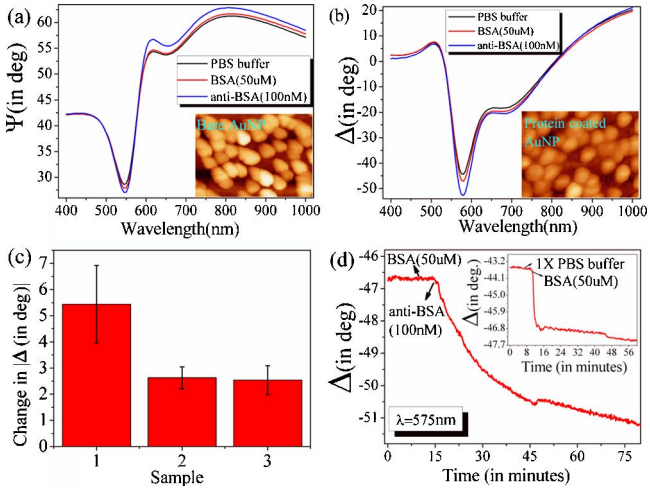

Fig. 3. (Color online) Spectral response of the ellipsometric parameters for (a) Ψ and (b) Δfor various configurations with respect to the addition of BSA and anti-BSA; (c) reproducibility of the measurement on three different samples and error bar over three different regions on the sample surface [atomic force microscopy images of the AuNPs with uncoated and coated biomolecules are shown in insets in (a) and (b)]. (d) Dynamic response of Δ.

and 100 nM, respectively. Ellipsometry signals, Ψ and Δ, of AuNPs were measured upon subsequent injections of PBS buffer solution and BSA and anti-BSA proteins. Because of the physisorption of BSA on the AuNPs surface, BSA protein will form a coating on the surface. The BSA solution is kept in the microfluidic cell for 1 h in order to obtain sufficient BSA coverage on the gold surface, followed by washing with PBS buffer to remove unbound proteins. Finally, anti-BSA protein was injected into the microfluidic cell and kept for 3 – 4 h to undergo protein–protein interaction, followed by washing with PBS buffer to wash away the unbound anti-BSA. Figures 3(a) and 3(b) show the spectroscopic responses for Ψ and Δ for AuNPs, covered by BSA, and then by anti-BSA. Figure 3(c) shows the reproducibility of the results with error bars for three different samples over different regions of the sample surface at 575 nm.

Figure 3(d) shows the real-time kinetic behavior of the interaction of anti-BSA with AuNPs covered by BSA, while the inset shows the interaction of BSA with AuNPs prior to the addition of anti-BSA. Surface morphology is very different for bare and protein (BSA + anti-BSA) coated AuNPs surfaces as shown in the insets of Figs. 3(a) and 3(b). With the addition of 100 nM concentration anti-BSA protein the phase signal (Δ) shows an increment (absolute value) of 5.691°. For a phase measurement accuracy of about 0.001°, the biomolecular detection limit of the proposed AuNPs-enhanced ellipsometric sensor by using the phase signal is about 18 pM ($\sim 1.63 \times 10^{-6} \times 100\,\text{nM}/0.0093$).

In conclusion, we have presented a simple optical alignment of phase-sensitive LSPR biosensors using AuNPs-enhanced ellipsometry. Through studies of BSA and anti-BSA molecular interactions, we have experimentally demonstrated both spectroscopic and dynamic measurement capabilities to sense high-affinity bimolecular interactions by using ellipsometry without labeling. This finding allows us to improve significantly the detection sensitivity of the biosensor without expensive nanofabrication techniques. We envision that this highly sensitive sensing platform can be used as a label-free optical detection technique for cancer cell diagnosis.

This work was supported by Academia Sinica, Taiwan, and by the National Science Council of Taiwan (NSCT) under contracts NSC 98-2112-M-001-022-MY3 and NSC 98-3112-B-001-022.

References

1. R. A. Sperling, P. R. Gil, F. Zhang, M. Zanella, and W. J. Parak, Chem. Soc. Rev. **37**, 1896 (2008).
2. P. Baptista, E. Pereira, P. Eaton, G. Doria, A. Miranda, I. Gomes, P. Quaresma, and R. Franco, Anal. Bioanal. Chem. **391**, 943 (2007).
3. I. H. El-Sayed, X. Huang, and M. A. El-Sayed, Nano Lett. **5**, 829 (2005).
4. N. Nath and A. Chilkoti, Anal. Chem. **76**, 5370 (2004).
5. M. M. Miller and A. A. Lazarides, J. Phys. Chem. B **109**, 21556 (2005).
6. T. Okamoto, I. Yamaguchi, and T. Kobayashi, Opt. Lett. **25**, 372 (2000).
7. A. V. Kabashin, S. Patskovsky, and A. N. Grigorenko, Opt. Express **17**, 21191 (2009).
8. W. K. Kuo and C. H. Chang, Opt. Express **18**, 19656 (2010).
9. V. G. Karvets, F. Schedin, A. V. Kabashin, and A. N. Grigorenko, Opt. Lett. **35**, 956 (2010).
10. H. Fujiwara, *Spectroscopic Ellipsometry: Principles and Applications* (Wiley, 2007).
11. G. Frens, Nature **241**, 20 (1973).
12. N. L. Dmitruk, T. R. Barlas, O. S. Kondratenko, and V. R. Romanyuk, Mater. Sci. Eng., C **23**, 159 (2003).
13. J. Homola, S. S. Yee, and G. Gauglitz, Sens. Actuators B **54**, 3 (1999).
14. J. Y. Lee, T. K. Chou, and H. C. Shih, Opt. Lett. **33**, 434 (2008).
15. A. N. Grigorenko, P. I. Nikitin, and A. V. Kabashin, Appl. Phys. Lett. **75**, 3917 (1999).